Journal of Materials Chemistry B

ROYAL SOCIETY OF CHEMISTRY

PAPER

View Article Online
View Journal | View Issue

Cite this: J. Mater. Chem. B, 2026, 14, 4080

Injectable oligomer-cross-linked chitosan hydrogels for biomedical applications

Iram Maqsood,*[ab] Hafiz Awais Nawaz,[ac] Ketpat Vejjasilpa,[a] Caroline Kohn-Polster,[a] Jan Krieghoff,[a] Alexandra Springwald,[a] Michaela Schulz-Siegmund[a] and Michael C. Hacker*[ad]

Injectable chitosan hydrogels, designed to emulate the extracellular matrix (ECM) in tissue engineering, are conventionally formed through physical gelation. This study aims to enhance stability and broaden the range of gel properties by adopting a covalent cross-linking approach. To achieve this, a series of hydrophilic oligomeric oligomers were synthesized, incorporating acryloyl morpholine (AMo) and reactive maleic anhydride (MA) in varying ratios, both with and without the hydrophobic comonomer pentaerythritol diacrylate monostearate (PEDAS). These oligomers, characterized by low molecular weight (M_n < 5000 Da) and differing anhydride content, were rheologically assessed for their ability to cross-link chitosan under physiological conditions. The resulting injectable oligomer-cross-linked chitosan hydrogels (iCsgel) exhibited substantial elastic strength (with an estimated E of up to 28 kPa). Furthermore, oligomer-cross-linking facilitated the production of chitosan-based hydrogels with customizable mechanical properties, controllable swelling behavior, and regulated degradation kinetics. Importantly, cell–laden iCsgel demonstrated excellent cytocompatibility and supported cell proliferation. As a proof-of-concept, some oligomers were partially modified with a fluorescent dye before the cross-linking process, resulting in decorated iCsgel. In summary, the established injectable oligomer-cross-linked chitosan hydrogels represent a promising platform with tunable material properties, making them well-suited for applications in tissue engineering and various biomedical fields, including bioprinting.

Received 28th October 2025,
Accepted 8th March 2026

DOI: 10.1039/d5tb02401c

rsc.li/materials-b

Introduction

Injectable hydrogels play a pivotal role in biomedical applications due to their minimally invasive administration, high water content, porous structure, and the ability to support live cells, facilitating the transport of nutrients and oxygen.[1,2] Macromolecules that form *in situ* gels can yield hydrogels that closely replicate the microarchitecture, mechanical properties, and functionalities of the extracellular matrix (ECM).[3] Chitosan, characterized by its innate antibacterial properties, bioactivity, biocompatibility, biodegradability, and osteoconductivity, is a promising natural biomaterial for cartilage and bone tissue engineering.[4–6] Chitosan can be *in vivo* hydrolysed by lysozyme, with degradation rates dependent on its molecular weight, and the resulting degradation products are known to be non-toxic, non-carcinogenic, and non-immunogenic.[7,8]

Current chitosan cross-linking strategies remain limited by the intrinsic drawbacks of both physical and chemical approaches. Physical cross-linking methods (*e.g.*, sodium tripolyphosphate or β-glycerophosphate) typically produce mechanically weak and structurally heterogeneous networks that are sensitive to environmental pH and ionic strength, resulting in limited long-term stability and uncontrolled drug release profiles.[9–13] In contrast, chemical cross-linking strategies often rely on reactive agents such as glutaraldehyde, formaldehyde, glyoxal, or epoxy compounds,[14–17] which can compromise cytocompatibility due to residual reactivity and potential toxicity.[18,19] Moreover, these agents may reduce the availability of functional groups and provide limited control over gelation kinetics. Although genipin offers improved biocompatibility, it exhibits comparatively slow reaction kinetics and may interact undesirably with encapsulated therapeutics.[16,20,21] Collectively, these constraints restrict the mechanical robustness, cytocompatibility, and long-term performance of injectable chitosan hydrogels for biomedical and tissue engineering applications.[22,23]

[a] Institute of Pharmacy, Pharmaceutical Technology, Faculty of Medicine at Leipzig University, 04317 Leipzig, Germany
[b] Department of Pharmaceutics, School of Pharmacy, University of Maryland, Baltimore, Maryland 21201, USA. E-mail: imaqsood@rx.umaryland.edu; Tel: +1(443)794-3120
[c] Institute of Pharmaceutical Sciences (IPS), University of Veterinary & Animal Sciences (UVAS), Abdul Qadir Jillani road, Lahore, Pakistan
[d] Heinrich Heine University Düsseldorf, Faculty of Mathematics and Natural Sciences, Institute of Pharmaceutics and Biopharmaceutics, 40225 Duesseldorf, Germany. E-mail: michael.hacker@hhu.de; Tel: +49 211 8114385

Our group has previously developed reactive maleic anhydride-containing ter-oligomers capable of efficiently cross-linking amine-bearing biomacromolecules for the fabrication of hydrogels and microstructured scaffolds in regenerative applications.[24,25] Upon copolymerization, maleic anhydride forms pendant succinic anhydride units along the oligomer backbone, which exhibit high reactivity toward nucleophilic amines.[26,27] Nucleophilic ring opening of the anhydride yields stable amide bonds while simultaneously generating a carboxylate group, thereby converting cationic amines into negatively charged moieties and contributing to network stabilization.[28]

Compared to aldehyde- or genipin-mediated cross-linking, anhydride chemistry enables rapid and controllable amine–anhydride conjugation under mild aqueous conditions. Importantly, anhydrides are transiently reactive and are converted into stable amide linkages without persistent cross-linker species, thereby minimizing residual reactivity and improving cytocompatibility. These features render anhydride-based systems particularly attractive for injectable, cell-compatible biomaterials.[29,30]

To address the need for injectable delivery, cytocompatibility, precise mechanical attributes, and controlled degradation, improvements were required to enhance the hydrophilicity of anhydride-containing oligomers. The objective of this study was to design a cytocompatible, hydrophilic oligomeric macromer incorporating reactive anhydride groups capable of covalently cross-linking chitosan under physiological conditions to meet injectability requirements, enabling cell encapsulation upon gelation. The ultimate aim is the application of injectable, cell–laden, oligomer-cross-linked chitosan hydrogels for regenerative purposes. A material design based on established free radical polymerization chemistry was employed to control the physico-chemical properties of the oligomeric oligomers by varying the comonomer type and ratio. Hydrophilic oligomeric oligomers were synthesized from acryloyl morpholine (AMo) to enhance hydrophilicity, maleic anhydride (MA) to introduce reactivity toward macromolecule amines, and pentaerythritol diacrylate monostearate (PEDAS) to enhance cohesion between polymeric chains and cell-material interaction, thereby strengthening the resulting hydrogel. These hydrophilic oligomeric oligomers are denoted as oPMoMA-*x* {oligo(PEDAS-*co*-AMo-*co*-MA)}, where *x* represents the MA molarity relative to one mole of PEDAS. Additionally, PEDAS-free oligomers were synthesized and designated as oMoMA-*x* {oligo(AMo-*co*-MA)}.

In our previous studies, we developed hydrophobic anhydride-containing oligomeric macromers for cross-linking gelatine in two-component hydrogel systems, establishing a modular and adaptable platform chemistry. These oligomers incorporated maleic anhydride to provide reactive anhydride functionalities, PEDAS to enhance mechanical cohesion and bio-interactivity, and a third comonomer to tailor physicochemical properties while suppressing maleic anhydride homopolymerisation. The first generation employed *N*-isopropylacrylamide (NiPAAm) to introduce thermo-responsive behaviour, yielding oPNMA-*x* {oligo(PEDAS-*co*-NiPAAm-*co*-MA)}.[24] In the second generation, NiPAAm was replaced by diacetone acrylamide (DAAm), introducing carbonyl functionalities to expand bioconjugation potential and producing oPDMA-*x* {oligo(PEDAS-*co*-DAAm-*co*-MA)}.[25]

In contrast to these earlier hydrophobic systems designed for gelatine-based matrices, the present study focuses on highly hydrophilic, low-molecular-weight oligomers specifically optimized for rapid injectable cross-linking of chitosan under physiological conditions. These platforms enable the creation of diverse gel compositions that differ in chemical makeup, peptide content, and mechanical attributes, with some being readily processable, forming stable monolithic gels. These anhydride group-bearing oligomers have been successfully applied to create hydrogels with various materials, including PEG–amines,[24] different gelatine fractions,[25,28,31] gelatine microparticles,[31] tubular conduits[32,33] and peripheral nerve regeneration.[34]

In current study, several hydrophilic oligomers, namely, oPMoMA-*x* and oMoMA-*x* with varying anhydride content were synthesized and characterized. The anhydride content and molecular weight per anhydride group determine the hydrogel cross-linking density, allowing for tuneable properties within a suitable range. Injectable covalently cross-linked chitosan hydrogel (iCsgel) was fabricated from these novel, low molecular weight hydrophilic oligomers upon reaction with chitosan. The resulting hydrogels were characterized concerning their composition, microarchitecture, porosity, and mechanical strength. Importantly, the cytocompatibility of cell–laden iCsgel was extensively investigated. The effect of oligomeric oligomer chemistry and cross-linking ratio on swelling and degradation properties of hydrogels was examined in comparison to a physically assembled chitosan gel.

In our two-component hydrogels, bioconjugation with amine-bearing molecules is easily achievable by decorating these molecules on the oligomer in solution, maintaining a defined stoichiometric ratio for amide linkage conjugation while retaining anhydrides for subsequent hydrogel formation. A similar approach was applied to injectable chitosan-based gel formulations using the fluorescent dye 6-aminofluorescein (6-AF) as a model substance.

Materials and methods

Acryloyl morpholine (4-acryloyl morpholine, AMo), pentaerythritol diacrylate monostearate (PEDAS), 2,2′-azobis(2-methylpropionitrile) (azobisisobutyronitrile, AIBN), 6-aminofluorescein (6-AF), 2,4,6-trinitrobenzenesulfonic acid (TNBS), Dulbecco's modified Eagle's medium (DMEM) low glucose (with and without phenol red), dimethyl sulfone (DMS), chitosan (low molecular weight, M_w 50–190 kDa, degree of deacetylation: 75–85%) were purchased from Sigma-Aldrich (Seelze, Germany). Tetrahydrofuran (THF) was obtained from VWR BDH Prolabo (Darmstadt, Germany), refluxed over sodium and potassium, and freshly distilled before use. Deuterated chloroform ($CDCl_3$) was obtained from Armar Chemicals (Leipzig, Germany). Diethyl ether, dichloromethane, β-glycerol phosphate (β-GP), phosphate buffered saline (PBS) and hydrochloric acid (HCl) 37% were purchased from AppliChem (Darmstadt, Germany). Foetal bovine

serum (FBS), penicillin/streptomycin (P/S), and trypsin were purchased from PAA Laboratories (Pasching, Austria). AlamarBlue™ reagent, ethidium homodimer-1 (EthD-1), and calcein-acetoxymethyl (calcein-AM) were obtained from Invitrogen (Darmstadt, Germany). WST-8 assay reagent (Rotitest® Vital) was provided by Carl Roth GmbH (Karlsruhe, Germany). Anhydrous dimethyl sulfoxide (DMSO) was obtained from Life Technologies (Darmstadt, Germany). Maleic anhydride (MA) and 1,2-propanediol (+99% propylene glycol (PG)) were obtained from Acros Organics (Geel, Belgium). Glucose monohydrate and 4′,6-diamidino-2-phenylindole dihydrochloride (DAPI) was purchased from Merck (Darmstadt, Germany). Deionized, ultrapure water as used for all experiments was produced by a Milli-Q® purifier system (Millipore Elix 10, Schwalbach, Germany).

Oligomer synthesis

Novel oligomers, referred to as oPMoMA-*x* {**o**ligo(**p**entaerythritol diacrylate monostearate) (PEDAS)-*co*-acryloyl **mo**rpholine (AMo)-*co*-**m**aleic **a**nhydride (MA)}, were synthesized *via* free radical copolymerization of the comonomers PEDAS, AMo, and MA (see Fig. 1A).[24] The molar ratio of PEDAS to AMo + MA in the synthesis feed was kept at 1 : 20, while the MA reaction feed relative to PEDAS varied between 2 and 10. The reaction involved dissolving the appropriate amounts of comonomers in dried THF and initiating copolymerization with AIBN (2% n/n) at 60 °C under a nitrogen atmosphere. After 18 hours, the synthesized polymer was concentrated and precipitated with diethyl ether. The resulting polymer was vacuum-dried under ambient conditions and subjected to chemical characterization.

Similarly, hydrophilic oligomers without PEDAS {**o**ligo(**AMo**-*co*-**MA**)} (referred to as oMoMA-*x*)(see Fig. S1A), as well as previously established hydrophobic oligomers, oPNMA-*x* {**o**ligo(**P**EDAS-*co*-***N***-isopropylacrylamide(NiPAAm)-*co*-**MA**)}[24,31] and oPDMA-*x* {**o**ligo(**P**EDAS-*co*-**d**iacetone acrylamide(DAAm)-*co*-**MA**)},[25] were synthesized through free radical copolymerization of the monomers. PEDAS-free hydrophilic oligomer (named as) oMoMA-*x* have been synthesized by free radical copolymerization of the comonomers AMo and MA. Briefly, the co-monomer combination of 20 co-monomers was kept constant, out of which *x* represent MA in oMoMA. The co-monomers were dissolved in dried THF, and free-radical copolymerization was initiated with AIBN (2% n/n) at 60 °C under an inert atmosphere. The resulting oligomers were concentrated and precipitated with diethyl ether to remove THF completely and were vacuum-dried before further chemical characterization.[24]

Chemical characterization

Verification of chemical composition of oligomers was accomplished through ^{1}H NMR and ^{13}C NMR spectra in $CDCl_3$, while polymerization confirmation was achieved *via* FTIR-ATR.

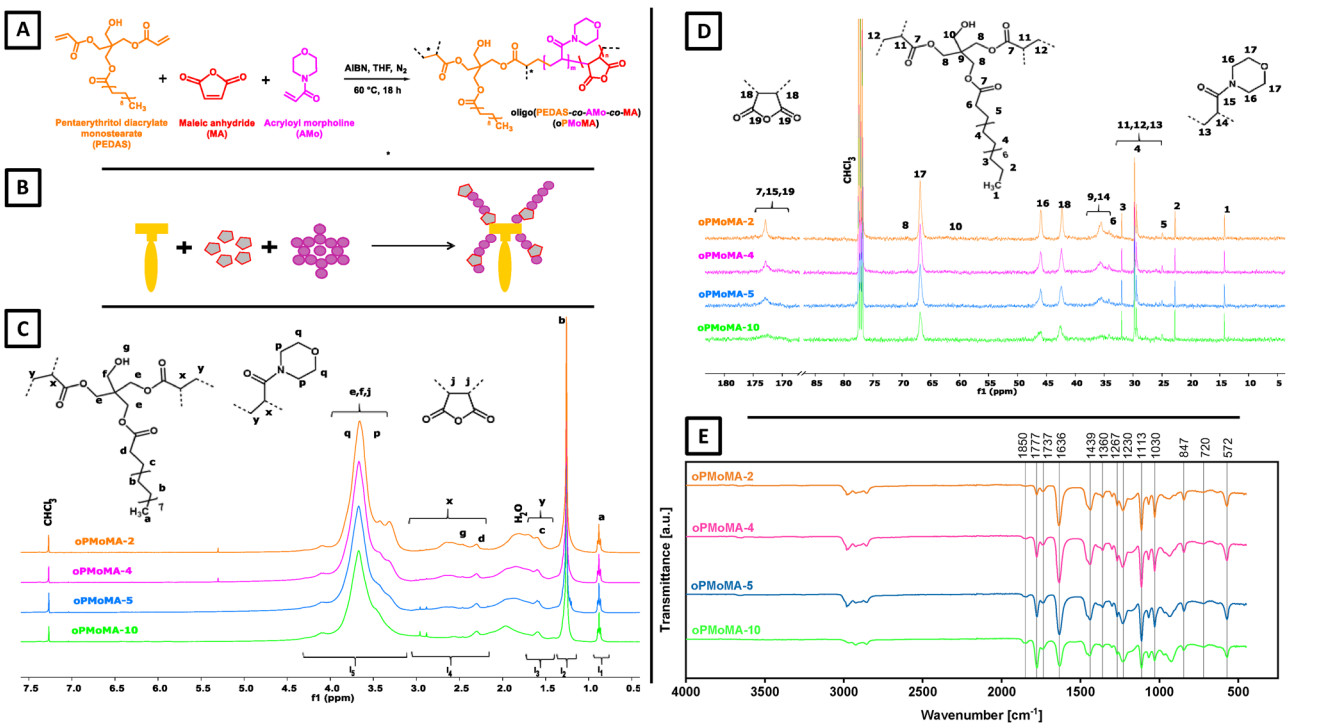

Fig. 1 Hydrophilic oligomeric cross-linkers synthesis scheme and NMR spectra. (A) Chemistry of oligomeric oligomers, oPMoMA {oligo(PEDAS-*co*-AMo-*co*-MA)} synthesized from PEDAS, AMo and MA by free radical polymerization (* indicates possible branching sites). (B) Illustration of oPMoMA-*x* synthesis. (C) Stacked ^{1}H NMR spectra of oPMoMA-*x*. The letters assigned to the peaks correspond to the protons at the positions labelled in the structural elements of the copolymers. I_1–I_5 represent the integrals used to determine oligomer composition. (D) Stacked, representative ^{13}C NMR spectra of oPMoMA-*x* of different MA feed. Peaks are labelled with digits representing specific carbons in respective the structural elements of the copolymers. (E) Fourier-transform infrared spectroscopy (FTIR) stacked spectra of hydrophilic oligomer oPMoMA-*x*.

Molecular weight distributions were determined using a SECurity GPC system relative to polystyrene standards as previously described. The obtained molecular weight characteristics were rounded to the nearest multiple of 50. Anhydride content was determined *via* conductometric titration, and fractions of intact anhydrides were calculated using Brown-Fujimori titrations as detailed in previous studies.[24]

Chitosan pre-processing and cross-linking

A concentrated chitosan solution (3.3% in 0.1 N HCl) was autoclaved and subsequently diluted with Dulbecco's modified Eagle's medium (DMEM) low glucose culture medium (resulting chitosan concentration: 1.65%) under aseptic conditions. The pH was adjusted to a physiological value (pH 7.3) using a sterile 0.03 M β-glycerophosphate (β-GP) solution in culture medium at 2–8 °C under vigorous stirring and aseptic conditions (see Fig. 2A). To characterize the cross-linking reaction between the novel hydrophilic oligomers (oPMoMA-*x*) and chitosan at physiological temperature, rheological measurements were carried out. A thermostated oscillating rheometer equipped with a steel cone geometry at 37 °C was used. The cross-linking reaction was initiated by mixing the pH-adjusted chitosan solution with the oPMoMA-*x* solution (40%) in a 7 : 3 (v/v) mixture of DMSO and propylene glycol. The solutions of chitosan and oligomer were individually dispensed onto the rheometer plate before the gap was closed, and the measurement was started. Cross-linking commenced immediately upon contact of the solutions. Mixing was supported by an initial 720° rotation of the upper geometry within 10 seconds. A time sweep experiment was conducted to analyse storage modulus (G'), loss modulus (G''), and complex viscosity (η^*) at a frequency of 1 Hz for over 30 minutes. Control time sweep experiments were also performed using a blank chitosan solvent to evaluate the chemical cross-linking ability of the oligomers *via* reaction with available free amines of chitosan, forming amide bonds. Rheological measurements were also conducted to investigate viscoelastic behaviour differences between pristine and autoclaved chitosan solutions at 20 and 32 °C.

Injectable oligomer-cross-linked chitosan hydrogel (iCsgel) fabrication

ICsgel were fabricated *in situ* by cross-linking pH-adjusted chitosan (Cs) solution (1.65%) with anhydride-containing oligomers (oPMoMA-*x*). L929 mouse fibroblast cells (Cell Lines Service, Eppelheim, Germany) at passage 39–41 were aseptically dispersed at a density of 100 000 cells/50 μL of chitosan solution and the dispersion was subsequently cross-linked with oligomer solution (40% in DMSO and PG (7 : 3 v/v)) to fabricate cell–laden iCsgel. Blank (cell-free) iCsgel and physically gelled (gelation by pH adjustment without addition of oligomer) chitosan gels were fabricated as control materials. The resulting gels were incubated (37 °C, 5% CO_2) in culture medium or PBS for cytocompatibility experiments or to determine

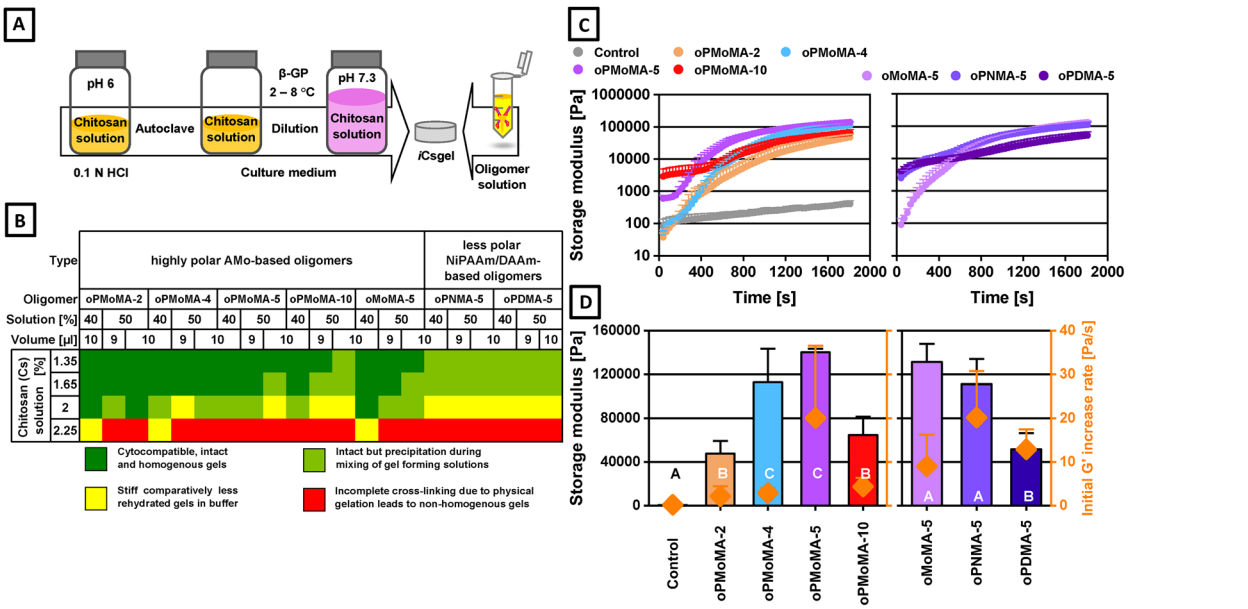

Fig. 2 (A) Schematic illustration of pre-processing of gel forming solutions including low molecular weight (LMW) chitosan and oligomer solution chitosan hydrogel fabrication. (B) Heatmap indicating hydrogel quality of all investigated iCsgel using both components chitosan solution (100 μL) and oligomer in different concentration and volume. Data was obtained from different experiments and colour scale indicating overall gel quality based on formulation processability, efficiency of cross-linking and homogeneity of hydrogels. (C) Rheograms depicting reaction between chitosan and a series of hydrophilic oPMoMA-*x* oligomers (left image) and between chitosan and a set of MA-5-type oligomers (right image). Time sweeps profiles (logarithmic scale) of storage moduli (G') for cross-linking reaction with oPMoMA-*x* (2, 4, 5, 10), oMoMA-5, oPNMA-5 and oPDMA-5 in comparison to control mixtures (without oligomer). (D) For reasons of clarity, the last points of the profiles (G' at 1810 s) are plotted separately (columns, left *y*-axis) and initial rate of modulus (G') increase of each formulation (diamonds, right *y*-axis). Data points, columns, diamonds with error bars represent means ± standard deviations (n = 4). Columns with different letters are statistically significantly different ($p < 0.05$).

physicochemical properties. While the culture medium or PBS was replaced every 48 hours.

iCsgel characterization

Rheological characterization. The stiffness of iCsgel was determined through oscillating rheology at 37 °C, using an 8 mm steel plate with a 1.2 mm gap.[25,31] In brief, iCsgel discs (diameter: 8 mm) were fabricated in polypropylene moulds and incubated overnight with cell culture medium. Then the equilibrium swollen iCsgel discs were rheologically analysed using frequency sweep experiments (0.1 to 10 Hz), with measurements of storage modulus (G'), loss modulus (G''), and complex viscosity (η^*) at 1 Hz. All experiments were carried out in quadruplicate. The physicochemical properties of iCsgel, particularly leachables, water uptake, and dry weight after lyophilization, were evaluated.

Cross-linking degree. The degree of cross-linking in iCsgel was indirectly determined by assessing the residual free amino groups of chitosan using a TNBS assay, following established protocols.[25,31] In this procedure, iCsgel discs were fabricated as described above and were lyophilized and subjected to the TNBS reaction mixture (water and 4% sodium bicarbonate solution (4 : 1), pH 8.5). Under ambient conditions in dark, freshly prepared 0.5% TNBS solution was added and samples were incubated at 40 °C for 4 h. Afterwards, 18 mL of 6 N HCl were added to stop the reaction and stabilize the coloured reaction products and samples were incubated at 60 °C for another 1.5 h successively. The gels were transferred to 96 well plate, mechanically destroyed and 100 μL of respective reaction mixture was added to each well to quantify the cross-linking degree by measuring the formation of an orange-coloured conjugate using a plate reader at 346 nm against blank samples, which were prepared following the same procedure with the addition of HCl solution prior to TNBS solution addition.

Porosity and structural analysis. Porosity of iCsgel was determined using a solvent displacement method.[35] The volume and weight of lyophilized iCsgel were used to calculate porosity. Structural analysis of gold sputtered samples was done by scanning electron microscopy, and chemical characterization was performed with Fourier-transform infrared spectroscopy (FTIR-ATR).

Derivatization of oPMoMA-*x* and fabrication of derivatized hydrogels. In a proof-of-concept experiment, the fluorescent dye 6-aminofluorescein (6-AF) was covalently linked to oPMoMA-*x* through amidation. A portion of the intact maleic anhydride in the oligomers was derivatized with 6-AF to produce oPMoMA-$x^{+6\text{-AF}}$. The process started by dissolving the oligomer in the DMSO-PG-mix. 6-AF was dissolved in DMSO. These solutions were mixed and allowed to react for 3 hours with gentle shaking. The resulting fluorescently labelled oligomer was used to cross-link chitosan as previously described. The labelled iCsgel was then analysed using light and fluorescence microscopy, and the fluorescent intensity was measured using a plate reader. Control iCsgel were created using unmodified oligomers.

Cytocompatibility assessment. The cytocompatibility of iCsgel was evaluated according to the ISO 10993-5 standard. L929 mouse fibroblasts were cultured in DMEM low glucose with 10% FBS and 1% P/S at 37 °C and 5% CO_2. Prior to iCsgel fabrication, cells were detached, counted, and suspended in sterile chitosan solution. Aseptically, cell–laden iCsgel was cross-linked in small moulds submerged in culture medium. The medium was replaced every 48 hours. Osmolarity and pH of primary and secondary extracts (aspirated CM after 24 h and 72 h of cell encapsulation respectively), plain DMEM, serum-containing CM and PBS were measured.

Live/Dead® assay. Cell viability, morphology, and proliferation within iCsgel were assessed using a Live/Dead® assay. The cell–laden iCsgel was stained and imaged at different time points using a confocal laser scanning microscope.

AlamarBlue™ assay. To quantify cell viability, an AlamarBlue™ assay was performed at different time points. Initially, at defined time points (day 1, 3 and 7) cell–laden hydrogels were hydrated with sterile culture medium after washing with PBS under aseptic conditions. Subsequently, AlamarBlue™ reagent (10%) was added to each well in the dark and incubated at 37 °C under gentle shaking for 4 h. Afterwards, the colorimetric change (chemical reduction of resazurin (blue) to resorufin (red) by viable cells) was quantified using a fluorescence plate reader. As encapsulated cells in oligomer-cross-linked chitosan hydrogels are not directly accessible to dye and sample measurement was often inconsistent due to heterogeneous dye distribution, a consecutive AlamarBlue™ assay was also conducted. Briefly, L929 fibroblast cells were suspended into chitosan solution at the same density and in similar fashion as described above. AlamarBlue™ reagent was added to the cell suspended chitosan solution in small plastic moulds prior to cross-linking step. Subsequently, the cell- and dye–laden iCsgel were supplied with serum-containing CM after cross-linking under aseptic conditions and later incubated at 37 °C and 5% CO_2 under a humid atmosphere. The dye was freely diffused out of the gel and colour of CM turned red upon reduction of resazurin by viable cells. At day 1, 100 μL of supernatant CM was carefully aspirated under aseptic conditions and transferred to 96 well plate (BD Falcon™) and colorimetric change was quantified using Tecan Infinite F 200 plate reader (Salzburg, Austria) as mentioned above. Furthermore, the fluorescence intensities were also monitored by aspirating the supernatant at day 2 and 3 consecutively. All measurements were performed in quadruplicate.

WST-8 (Rotitest® Vital) assay. Cell viability and proliferation in iCsgel was also evaluated using WST (water-soluble tetrazolium salt) assay. cell–laden iCsgel was fabricated under sterile conditions as described above. cell–laden gels were scooped out of the moulds at defined time points (1, 3 and 7 days) after washing with PBS, smashed and transferred to 96 well plate under aseptic condition. Afterwards, 100 μL of DMEM and 30 μL of WST-8 reagent were added to each well and incubated at 37 °C + 5% CO_2 for 3 h under gentle shaking. The colorimetric changes in supernatant were monitored spectrophotometrically at 450 nm using Tecan plate reader. The blank

gels (cell-free) were also treated in the similar fashion to take the supernatant absorbance at 450 nm as control. All measurements were performed in triplicates.

SEM analysis of cell–laden iCsgel. Cell morphology and distribution were observed by scanning electron microscopy. Samples were fixed, dehydrated, and lyophilized before imaging.

***In vitro* degradation of iCsgel.** ICsgel were fabricated as described above and hydrogels were incubated in well-plates with PBS (pH 7.4) containing 0.01% sodium azide at 37 °C. Physically gelled chitosan discs were used as control and were treated in an analogous manner as oligomer cross-linked hydrogels. The medium of hydrogels was replaced with fresh PBS twice a week and every week the pH of aspirated medium was monitored. ICsgel was evaluated for leachables, equilibrium water content, swelling ratio, and remaining dry weight during a 42-day degradation study in preserved PBS. Samples were collected at defined time points, weighed, and analysed for swelling behaviour.

Results and discussion

Synthesis and characterization of reactive, cytocompatible, hydrophilic oligomeric oligomers

We sought to develop cytocompatible, highly hydrophilic oligomeric oligomers for the purpose of creating injectable chitosan hydrogels. To achieve this, we employed acryloyl morpholine (AMo) as a hydrophilic comonomer and co-polymerized it with maleic anhydride (MA). We synthesized these hydrophilic oligomers with (Fig. 1) and without (Fig. S1) pentaerythritol diacrylate monostearate (PEDAS), that has been shown to improve hydrogel storage modulus, using free radical polymerization (Table 1 and Table S1) according to a previously established strategy.[25,31] The anhydride groups in the oligomers can later be used for covalently cross-linking nucleophilic amine-containing polymers like chitosan. AMo was chosen due to its non-ionic nature, solubility of its homopolymer in polar solvents, terminal unsaturation, and ability to form hydrogen bonds.[36] The inclusion of PEDAS, which features a long stearate chain, facilitates interactions with proteins within the hydrogel matrix and enhances hydrogel storage modulus through maintaining a hydrophilic–lipophilic balance.

Proton NMR (^{1}H NMR) data allowed for qualitative and quantitative of comonomer composition assessment according to previously published methodologies that use the fatty acid chain as internal reference. NMR spectroscopy analysis showed that the proton signals of the morpholine ring of AMo increased with the AMo feed (Fig. 1C). Determining the MA content from NMR was, however, challenging due to signal overlap with AMo. The use of dimethyl sulfone as an internal reference allowed us to quantify the AMo content in the absence of PEDAS (Fig. S1C). Carbon (^{13}C) NMR analysis further confirmed the successful incorporation of AMo, PEDAS, and MA in the oligomers (Fig. 1D and Fig. S1D).

The FTIR spectra exhibited characteristic peaks corresponding to the presence of cyclic anhydride, indicating the successful copolymerization of MA with other comonomers (Fig. 1E). The spectral data confirmed the co-polymerized MA-AMo structures (Fig. 1E and Fig. S1E).

The MA content in the oligomers was determined through acid–base titrations, further indicating efficient MA copolymerization. The oligomers demonstrated good control of MA content (Fig. S2A). The obtained GPC data of oligomers complemented the NMR results and demonstrated the adjustability of AMo and MA contents in small increments. Molecular weights (M_n) of hydrophilic oligomers ranged between 1550 and 4350 Da of oPMoMA-*x* and 1150 and 2050 Da of oMoMA-*x* respectively as revealed by GPC and an indirect correlation with MA feed (Fig. S2B and C) together with direct correlation with AMo feed (Fig. S2D and E) was found (Table 1 and Table S1). Hence, oligomers with adjustable MA contents and average molecular weights (M_n) below 5000 Da, which enable high cross-linking degrees and adaptable material engineering, could be synthesized following our previously established protocols.

In summary, the co-polymerization of PEDAS, AMo, and MA produced oligomers with low molecular weights ($M_n < 5000$ Da), aligning with previous findings. These low molecular weights are advantageous for creating versatile, cross-linked hydrogels that ensure renal eliminability after hydrogel degradation. As biological building blocks, we previously used gelatine or gelatinous peptides. In this study, we intended to fabricate chitosan hydrogels with tuneable properties using these adjustable, low molecular weight oligomers. We consider these hydrophilic oligomers with anhydride functionalities better cytocompatible as compared

Table 1 Compositions and chemical properties of synthesized oPMoMA-*x* {oligo(PEDAS-*co*-AMo-*co*-MA)} oligomers with different MA feeds

Oligomer type	Oligomer composition								Molecular weight (GPC)		
	Reaction feed (molar ratio)			AMo content [^{1}H NMR]		MA content [Titration]					
	PEDAS	AMo	MA	[AMo][a] per PEDAS	AMo[b] [wt%]	[wt%]	Per PEDAS	Intact MA[c] [%]	M_n [Da]	M_w [Da]	$Đ_M$
oPMoMA-2	1	18	2	18.69	86.6	5.7	1.89	97.2	4378 ± 68	14924 ± 147	3.41 ± 0.02
oPMoMA-4	1	16	4	17.79	78.5	12	3.87	96.2	3108 ± 18	8917 ± 37	2.87 ± 0.02
oPMoMA-5	1	15	5	16.84	76.2	13.4	4.25	93.4	2976 ± 12	8861 ± 11	2.98 ± 0.02
oPMoMA-10	1	10	10	13.80	66.1	20.5	6.07	93.8	1524 ± 20	3379 ± 58	2.22 ± 0.02

[a] Molar AMo content per mol of PEDAS. [b] Calculated total AMo weight [wt%] as determined by ^{1}H NMR analysis. [c] Anhydride intactness (fractions of chemically intact anhydride) and total anhydride content of oligomers expressed as weight percent [wt%] calculated from acid–base titrations. Number average molecular weight (M_n), weight average molecular weight (M_w), and molecular weight dispersity ($Đ_M = M_w/M_n$).

to the commonly used cross-linking agent glutaraldehyde. In contrast to aldehydes, anhydrides rapidly lose their residual chemical reactivity in aqueous environments, making them suitable for injectable hydrogel formulations. Additionally, the physicochemical properties of these two-component hydrogels will depend on both the biological component, chitosan, and the cross-linking oligomer. We are especially interested to tailor the mechanical properties through the choice of oligomer.

Cross-linking reaction with chitosan

A low molecular weight chitosan (50–190 kDa), obtained by alkaline deacetylation of chitin to a high deacetylation degree (~80%), was selected for its biocompatibility, antibacterial properties, and biodegradability. The initial chitosan solution (3.3%) was subsequently diluted to a desired concentration (1.65%) with culture medium under aseptic conditions. The pH of the solution was adjusted to the physiological range using a sterile β-glycerophosphate solution (0.03 M) at low temperatures (2–8 °C) and vigorous stirring (Fig. 2A). Beta-glycerophosphate (β-GP) has been extensively used with chitosan to form physical hydrogels at 37 °C through ionic interactions under certain critical conditions, such as a concentration of more than 2% to achieve chain entanglement.[12] Due to the free diffusibility of β-GP, it is considered a proton acceptor and not a divalent electrostatic cross-linker of chitosan amine groups.[37] The phosphate base can also serve as a source of organic phosphate for bone mineralization and for osteogenic differentiation.[38] Later, the above-mentioned pH adjusted chitosan solution was cross-linked with oligomer solution to fabricate iCsgel (Fig. 2A).

Steam sterilization-induced reduction in chitosan solution viscosity motivated a rheological evaluation using a cone plate setup. Rheological characterization involved moduli and viscosity assessments obtained during oscillatory time and frequency tests at 20 °C and 32 °C (Fig. S3). A temperature of 32 °C instead of 37 °C was selected to analyse effects of cross-linking prior to any possible additive effect of physical gelation of neutralized chitosan at physiological temperature.

The observed minor viscosity decrease observed post sterilization is attributed to biopolymer hydrolytic depolymerization.[39,40] Initially, modulus and viscosity of pristine chitosan exceeded that of autoclaved chitosan. Over time, autoclaved chitosan manifested heightened values towards the experiment's conclusion, suggesting more homogenous distribution over the measurement gap due to the initially reduced viscosity. Both solutions exhibited a sharp decline in complex viscosity with rising frequency at 20 °C and 32 °C, while moduli displayed a plateau, indicating shear thinning and possibly thixotropic behaviour[41] (Fig. S3A–D). Overall, whether autoclaved or pristine, chitosan solutions exhibited more fluid-like behaviour at 32 °C, attributable to enhanced interactions among chitosan, β-GP, and water over time.[42]

The cross-linking reaction between anhydride-bearing hydrophilic oligomeric oligomers and chitosan was evaluated using oscillation rheology. Different molar ratios of chitosan and oligomer solutions were used to monitor the reaction rheologically (Fig. 2). Chitosan's total free amino groups were calculated, and it was found to have significantly more amino groups compared to gelatinous peptide used in previous studies (Table S2).[43] This is one of the reasons why oligomer-cross-linked chitosan gels exhibited higher storage moduli as oligomer-cross-linked gelatinous peptide gels presented in previous studies. A heatmap was constructed of all investigated iCsgel using both components chitosan solution (100 μL) and oligomer in different concentration and volume indicating hydrogel quality based on formulation processability and efficiency of cross-linking (Fig. 2B). Hydrogel characteristics were influenced by the cross-linker type, solution concentration (40–50%), and chitosan content (1.35–2.25%), resulting in stable and uniform gels. ICsgel exhibited transparency at low MA (≤ 5), whereas MA-10 formulations showed increased turbidity and slight shrinkage. Increased macromer hydrophobicity correlated with reduced transparency and more pronounced precipitation. The formation of transient polyelectrolyte complexes between chitosan and anhydride-containing oligomers likely contributed to the observed precipitates. Based on these preliminary evaluations, formulations containing 40% oligomer and 1.65% chitosan were selected for subsequent investigations.

The optimized chitosan solution (1.65 w/v%) cross-linking was evaluated with a set of previously established hydrophobic oligomers (oPNMA-5 and oPDMA-5) in addition to hydrophilic oligomers (oPMoMA-*x* and oMoMA-*x*) (Fig. 2 and Fig. S4). The rheological data revealed an increase in dynamic moduli, indicating the formation of cross-linked elastic hydrogels with all tested oligomers (Fig. 2). The effect of the cross-linking group ratio ([MA]/[NH_2]) on the reaction kinetics was examined (Fig. 2C). The cross-linking reaction progressed more rapidly for oPMoMA-4 and -5 ([MA]/[NH_2] ratios of 0.59 and 0.64, respectively) as compared to other hydrophilic and hydrophobic oligomers. Hydrophobic oligomers showed higher initial storage moduli, possibly due to initial precipitation induced during mixing of hydrogel-forming solutions. Also, the hydrophobic and hydrophilic oligomers of higher anhydride content (MA = 10) demonstrated flatter gelation kinetic curves (Fig. S5). The control formulation without oligomers at 37 °C exhibited only a slight increase in moduli, likely due to transient physical gelation and increased chain entanglement. The rate of modulus increase was calculated from the reaction mixtures as a measure of the cross-linking reaction kinetics (Fig. 2D, right *y*-axis). Obviously, the rate increase was affected by relative anhydride content and molecular weight of oligomers. The rate was highest with the oPMoMA-5 oligomer, which provided the best balance of anhydride group density and chain mobility until viscosity increase. Network formation continued until the end of the oscillatory time test (30 minutes) and one could not determine time to modulus plateau from the measurements. All investigated oligomers induced rapid gelation, and the exact point of gelation (as crossover of G' and G'') was often quicker than the first values could be recorded.

The complex viscosities obtained during the cross-linking reactions indicated efficient network formation, with the hydrophilic oligomers containing MA-4 and MA-5 found to be the most optimal for hydrogel formation (Fig. 3). The low molecular

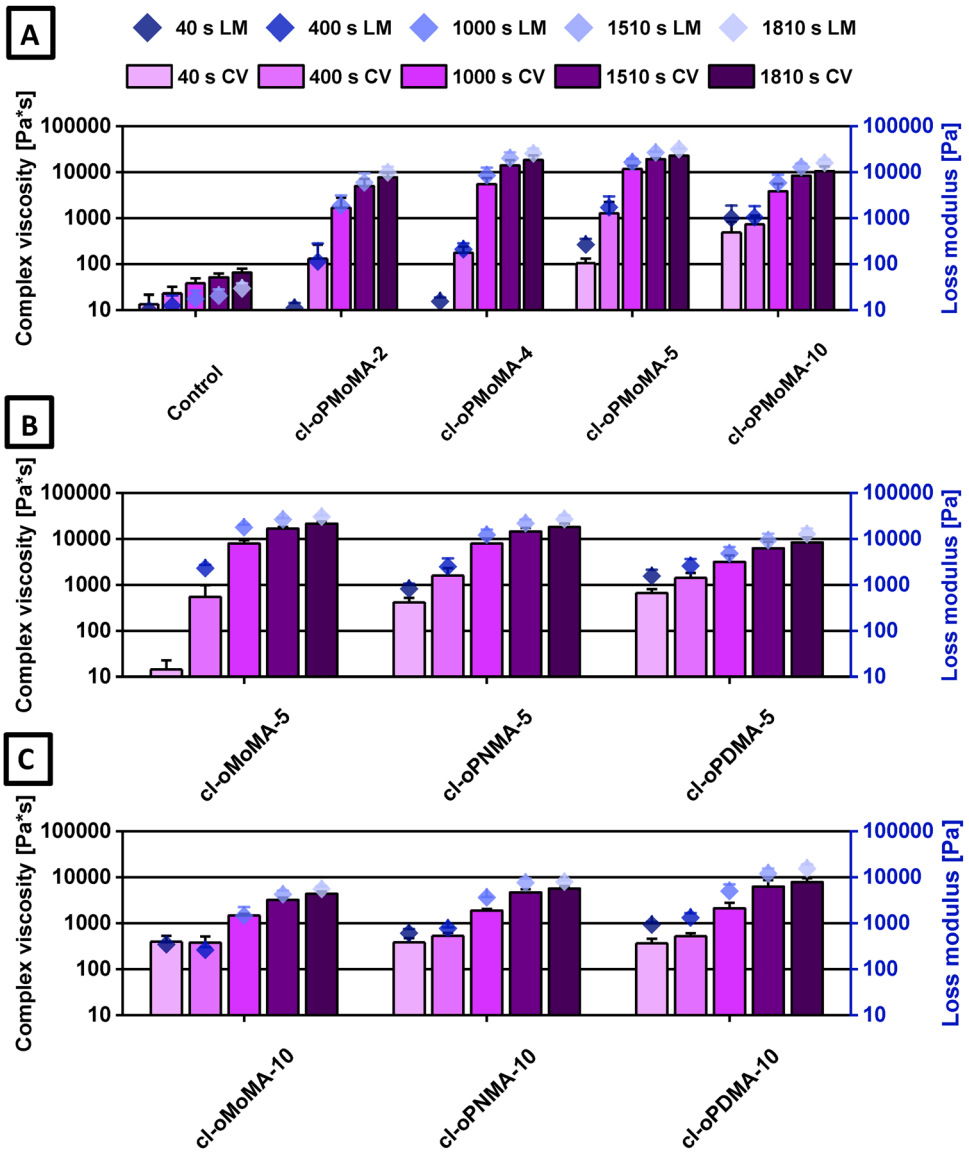

Fig. 3 Complex viscosities (η^*) (columns left y-axis) and loss modulus (G'') (diamonds, right y-axis) determined at different time points from rheological data as a measure of gelation kinetics after initiation of cross-linking reaction with various oligomers: (A) oPMoMA-x with different MA feeds in comparison to control, (B) different MA-5 oligomers, (C) different MA-10 oligomers. The corresponding storage moduli can be found in Fig. 2. Columns (complex viscosity) and data points (loss modulus) with error bars represent means ± standard deviations (n = 4).

weight oligomers served as efficient cross-linkers for chitosan, resulting in stable network formation. Overall, the study successfully demonstrated the efficient cross-linking of chitosan with hydrophilic and hydrophobic oligomeric anhydride-containing oligomers.

Injectable chitosan hydrogels (iCsgel) formation and characterization

Injectable chitosan hydrogels (iCsgel) were fabricated by *in situ* cross-linking of autoclaved pH-adjusted chitosan solutions with anhydride-containing oligomers by mixing 70 µL of 1.65% chitosan and 7 µL of 40% oligomer (10 : 1 ratio). The resulting hydrogels were homogeneous, stable, and transparent, with transparency decreasing as the oligomer's maleic anhydride (MA) content increased (Fig. 4).

To evaluate their mechanical properties, the storage moduli (G') of equilibrium-swollen hydrogels in culture medium at 37 °C were measured using frequency sweep oscillation rheology. An increase in hydrogel stiffness was observed with higher MA content (Fig. 4C). The apparent discrepancy in storage modulus for MA-10 gels between time-sweep (Fig. 2C) and frequency-sweep (Fig. 4C) measurements arises from differences in network maturation time. Rapid initial gelation constrained further modulus evolution within the 30-minute time-sweep experiment, whereas 24-hour equilibration in culture medium permitted continued amine–anhydride conjugation and equilibrium swelling. Under these conditions, the higher anhydride content of oPMoMA-10 yielded a greater cross-link density and consequently a higher

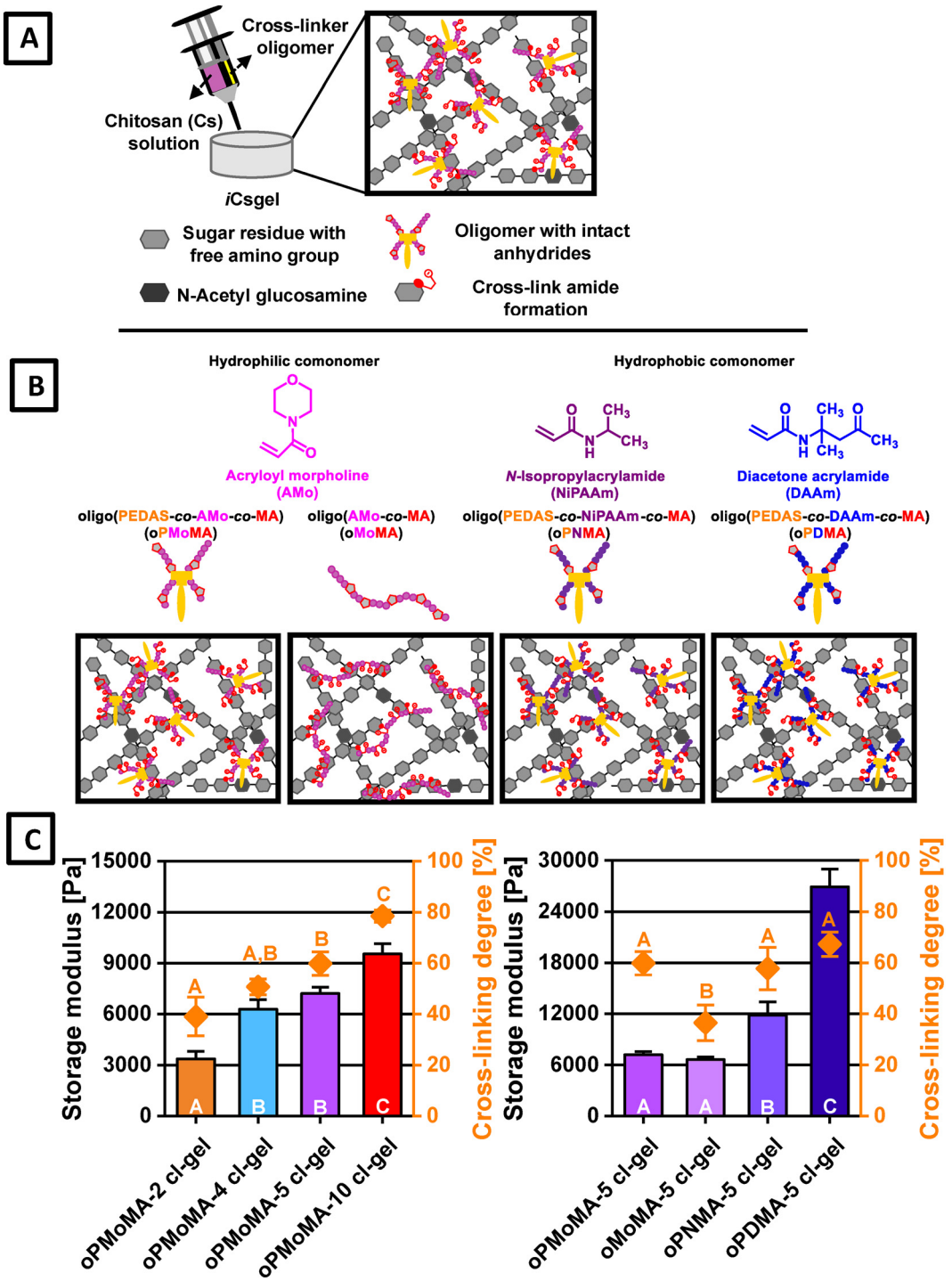

Fig. 4 (A) Schematic illustration of injectable oligomer-cross-linked chitosan hydrogel (iCsgel) fabrication (in the experiments the volumes were combined with two pipettes and not with a two-component syringe system as illustrated). (B) Schematic illustration of iCsgel fabrication (left to right) from hydrophilic oligomers oPMoMA-*x*, oMoMA-*x* and from conventional hydrophobic oligomers oPNMA and oPDMA. (C) Storage moduli (G') as determined from equilibrium-swollen (in culture medium) discs of iCsgel cross-linked with oPMoMA-*x* of increasing MA feed (left image) and with MA-5-type oligomers of different comonomer composition, all at 37 °C and 1 Hz (frequency sweep rheology). Cross-linking degrees (orange diamonds, right *y*-axis) as determined for lyophilized discs of corresponding formulation. Columns (storage modulus) and data points (cross-linking degree) with error bars represent means ± standard deviations (n = 3–4). Columns and data points with different letters are statistically significantly different, $p < 0.05$.

equilibrium storage modulus compared to oPMoMA-4 and -5 cross-linked gels.

The storage moduli values for iCsgel cross-linked with oPMoMA-*x* oligomers ranged from 3.4 to 9.5 kPa. These values

are in the range of mechanical moduli of soft tissues.[44] Gel modulus increased in the order: oMoMA < oPMoMA < oPNMA < oPDMA regarding the oligomer type of the iCsgel composition.

Cross-linking density, expressed as 30–80% amine conversion, was quantified using a TNBS assay, revealing a significant increase with higher MA content (Fig. 4C, right *y*-axis). The best formulations had around 60% cross-linking degree. Physicochemical properties, such as water content, dry weight, and leachables, were assessed (Fig. S6). ICsgel with lower MA content absorbed more water than those cross-linked with MA-10 oligomers but less than non-cross-linked chitosan gels. There was an inverse correlation between water content, dry weight, and cross-linking degree, as observed in previous research.[31] Furthermore, hydrogels with higher MA content had fewer leachables (Fig. S6).

For tissue engineering application, injectable hydrogels should be porous materials with open and interconnected networks to allow cell migration, cell proliferation, nutrient delivery and waste elimination.[45] The porosity assessment of iCsgel cross-linked with oPMoMA-*x* was conducted by liquid displacement method and the results are summarized in Fig. 5.[35] All tested chitosan hydrogels exhibited porosity in the range of 80–90%, irrespective of cross-linking degree and elastic strength (Fig. 5B). The highly porous, interconnected and homogenous microstructure of lyophilized iCsgel was also confirmed by scanning electron microscopy without considerable differences between the investigated formulations (Fig. 5C).[46] For tissue regeneration applications appropriate pore size, porosity and water uptake ability are favourable attributes to provide some space to embedded cells, later cell adhesion, and proliferation.[47–49] An interesting phenomenon was that no direct correlation was found between the obtained porosity of iCsgel and equilibrium water content which agreed with previous investigations.[35]

FTIR-ATR analysis of iCsgel demonstrated significant changes compared to pristine chitosan spectrum (Fig. S7). Initially, a weak ionic interaction between chitosan and β-GP was evidenced by slight shifts in the $-NH_3^+$ band (~1550–1650 cm^{-1}) and phosphate stretching bands (~900–1150 cm^{-1}) in iCsgel spectra. Further changes included a reduction in the broad absorption peak representing hydroxyl and amino groups, as well as the disappearance of the characteristic amide I peak of chitosan at 1650 cm^{-1}, replaced by a new peak at 1628 cm^{-1}. Additionally, the band at 1548 cm^{-1}, associated with the amino group of chitosan, vanished. The FTIR spectrum of cross-linked iCsgel displayed signals from both chitosan and oligomeric oligomers, with the absence of peaks assigned to the amino group of chitosan and the anhydride of the oligomer (1777 cm^{-1} and 1850 cm^{-1}). These observations indicated the successful amide formation (bands at 1628 cm^{-1}, 1445 cm^{-1}, 1235 cm^{-1} and 573 cm^{-1} representing –O═C–N [Amide I], primary amide [Amide VI], (NH) + (–O═C–N) [Amide III] and (C–C) + (–O═C–N) [Amide IV]) from anhydrides and amines yielding chemically cross-linked chitosan-based hydrogel.

Fluorescent labelling of iCsgel *via* cross-linking with derivatized oPMoMA-*x* was accomplished by covalently attaching 6-AF to the oligomer backbone through amide bond formation (Fig. 6A). The successful integration of the fluorescent probe was confirmed by ^{1}H NMR analysis (Fig. S8). Stereomicroscopic images showed a yellow coloration in the fluorescently labelled iCsgel, while the control iCsgel remained colourless. Fluorescence micrographs demonstrated a significant increase in fluorescence intensity in the labelled gel compared to the control (Fig. 6B–E). This increased fluorescence was attributed to the incorporation of fluorescently labelled oligomers. Surprisingly, oPMoMA-$10^{+6\text{-AF}}$ cross-linked iCsgel exhibited significantly higher fluorescence intensities among other derivatized (+6-AF) iCsgel, which confirmed the hypothesis of increasing fluorescence intensity with increasing amide bond formation (Fig. 6F). The fluorescence intensity increased with higher concentrations of derivatized oligomers as evident from labelled iCsgel cross-linked with oPMoMA-5 modified with different MA_{eq} of 6-AF (Fig. 6G). These findings open new possibilities for designing biomimetic hydrogels *via* derivatization with bioactive molecules.

Cell culture

In tissue regeneration, cell adhesion, proliferation, and differentiation are crucial for tissue development and are considered of fundamental importance for biomedical applications.[50] In this study, we assessed the cytocompatibility of cell–laden iCsgel, which is prerequisite for further application in tissue regeneration and biomedical therapies. Initially, we encapsulated L929 mouse fibroblast cells in the iCsgel and examined their behaviour over time (Fig. 7).[51] Confocal microscopy images revealed good cell viability, migration, and proliferation within the gel matrix. Initially, the cells had a rounded shape, but by day 7, increased cell spreading was observed (Fig. 7B). Cellularity and cell shape was supported by scanning electron microscopy (Fig. 7C). Overall, injectable formulations have shown good interaction with encapsulated cells, which can be attributed to the intrinsic biocompatibility of chitosan.[52] Quantitative analysis of metabolic activity of the cells using the AlamarBlue™ assay supported this data and displayed cell viability and proliferation with cultivation time (Fig. 7D). The analysed colorimetric changes after day 7 were significantly different from day 1 and 3[53], though no significant difference was revealed among iCsgel cross-linked with oPMoMA of different AM feeds. Osmometric measurements showed that osmolarity was not a limiting factor for cell viability within the gel (Fig. 7E).

Taken into consideration that encapsulated cells in oligomer-cross-linked chitosan hydrogels are not directly accessible to dye resulting in heterogeneous dye distribution and inconsistent measurement, a consecutive AlamarBlue™ assay was also conducted. A significant increase in fluorescence values was revealed in gel cross-linked with MA-4- and MA-5-type oligomers at day 3, however, in the gel cross-linked with oPMoMA-10, cellularity decreased due to the gels' high cross-linking density and rigid nature[54] (Fig. 7F). Regarding the analytical methodology, it is important to observe that gels without cells also showed significant fluorescence levels, suggesting a redox reaction between the material and dye, even when the material is cross-linked.

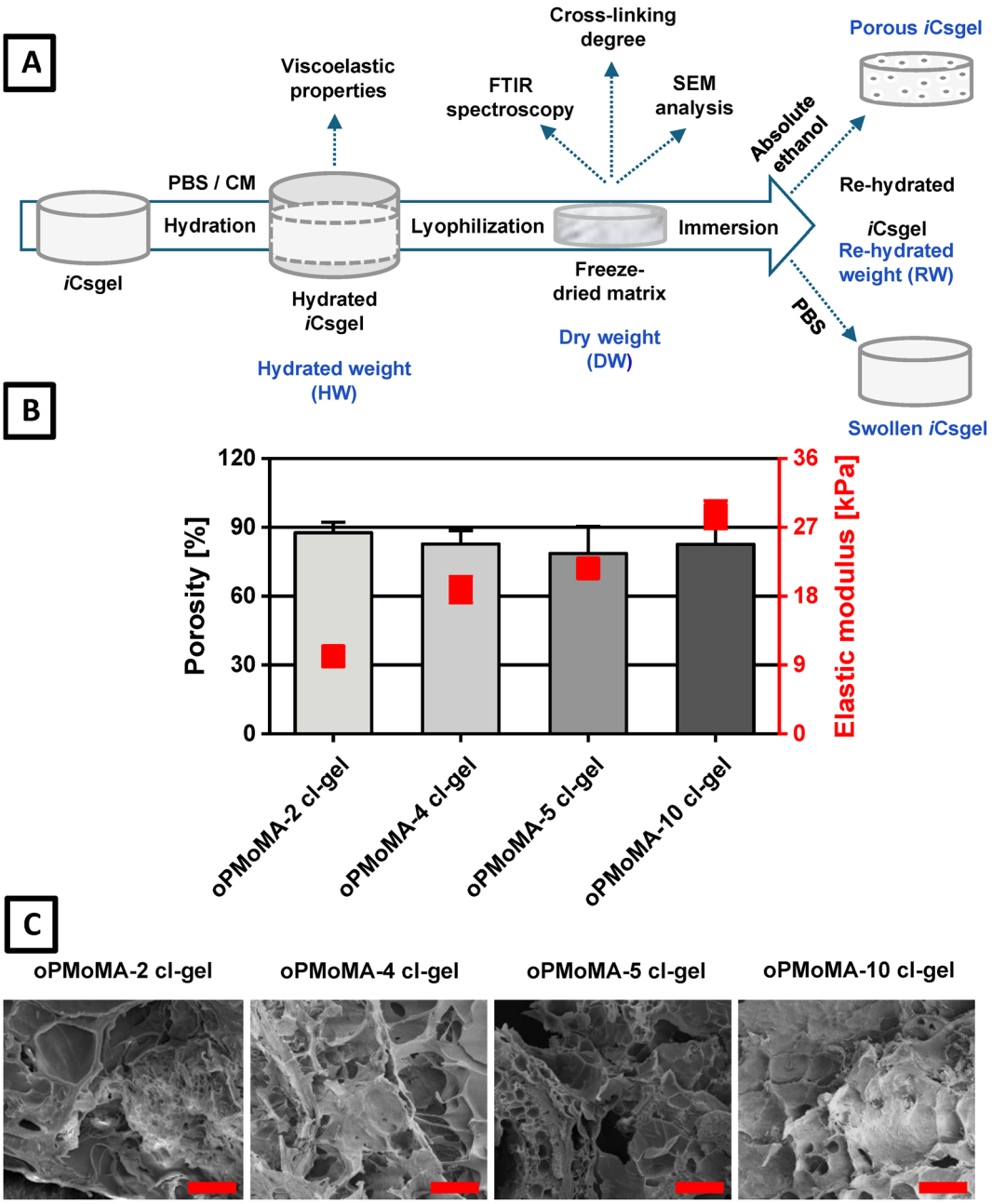

Fig. 5 (A) Illustration of different analyzed parameters of injectable chitosan hydrogels (iCsgel). Freshly fabricated iCsgel discs were hydrated in culture medium (CM) to determine storage moduli of hydrated hydrogels discs rheologically in equilibrium-swollen state. The hydrated iCsgel discs in phosphate buffered saline (PBS) were lyophilized to calculate leachables. From the obtained hydrated weight (HW) of equilibrium swollen iCsgel discs and dry weight (DW) of lyophilized discs, equilibrium water content was determined. The dried discs were weighed and a standard TNBS assay was conducted to determine the cross-linking degree of iCsgel. The structural analysis of iCsgel was done by scanning electron microscopy (SEM) and the dried iCsgel were pulverized prior FTIR analysis. The lyophilized discs were further immersed in PBS to calculate swelling ratio and in absolute ethanol to measure the porosity of iCsgel discs by solvent displacement. (B) Porosity of iCsgel cross-linked with oPMoMA-*x* as determined by solvent displacement method. Data points (right *y*-axis) represent elastic moduli (*E* estimated as 3*G*′) of iCsgel cross-linked with oPMoMA-*x*. Columns, data points with error bars represent means ± standard deviations (n = 4). (C) SEM analysis of iCsgel. Scale bars represent 50 μm.

In literature, the role of poly(ethylene-*alt*-maleic anhydride) as reduction catalyst has been discussed.[55] Also, reduction of resazurin to resorufin has been reported to occur by different means than viable cells, such as photo-reduction with several types of amines upon irradiation and plasmon-mediated reduction by hydroxylamine and gold nanoparticles.[56,57] Hence, we deduce that polymers containing polymerized maleic anhydride have the potential to reduce resazurin to resorufin even when the anhydrides have been amino- or hydrolysed.

We conducted additional experiments to encapsulate cells within gels cross-linked by different oligomers containing the same anhydride feed, here MA-5-type oligomers. Hydrophilic

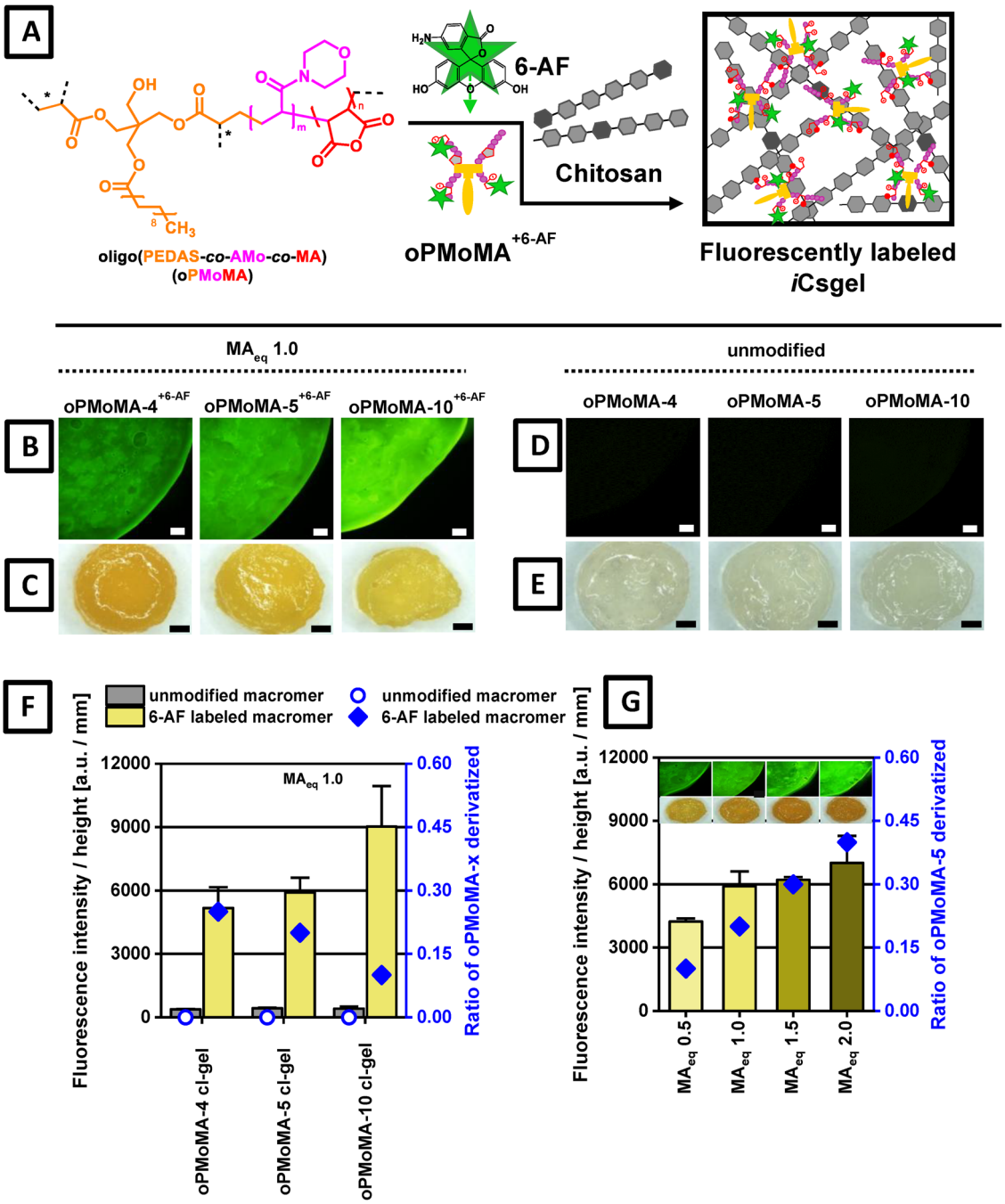

Fig. 6 (A) Schematic illustration of oPMoMA-*x* derivatization with 6-aminofluorescein (6-AF) and fabrication of strongly fluorescent iCsgel upon cross-linking with covalently derivatized oPMoMA-$x^{+6\text{-AF}}$. (B) Fluorescence micrographs (scale bars 250 μm) of labelled iCsgel cross-linked with derivatized oPMoMA-4, -5, -10 (1.0 MA_{eq} of 6-AF). The significantly higher fluorescence intensities at the gel boundaries are attributed to optical refraction effects. (C) Stereomicroscopic images of labelled iCsgel (scale bars 1 mm). (D, E) Fluorescent micrographs and photographic images of control iCsgel fabricated upon cross-linking with pristine oPMoMA-*x* (scale bars represent 250 μm and 1 mm respectively). (F) Thickness-normalized fluorescence intensities of labelled iCsgel as determined at 485 nm/528 nm (excitation/emission) using the Tecan plate reader, control (grey) and oPMoMA-*x* (MA_{eq} 1.0) labelled (yellow) cross-linked gels. (G) Labelled iCsgel cross-linked with oPMoMA-5 modified with different MA_{eq} of 6-AF. Columns with error bars represent means ± standard deviations (n = 3).

oligomers, oPMoMA-5 and oMoMA-5, cross-linked gels showed good cytocompatibility and increased cell numbers over time, while hydrophobic oligomer, oPNMA-5 and oPDMA-5, cross-linked gels led to significant cell death and inhibited proliferation (Fig. S9A).[58,59] The inhibition of cell proliferation in hydrophobic oligomers cross-linked iCsgel was also confirmed by AlamarBlue™ and WST-8 assay, which showed almost negligible dye conversion for iCsgel cross-linked with hydrophobic oligomers but very good cell viability and proliferation in cell–laden iCsgel cross-linked with hydrophilic oligomers

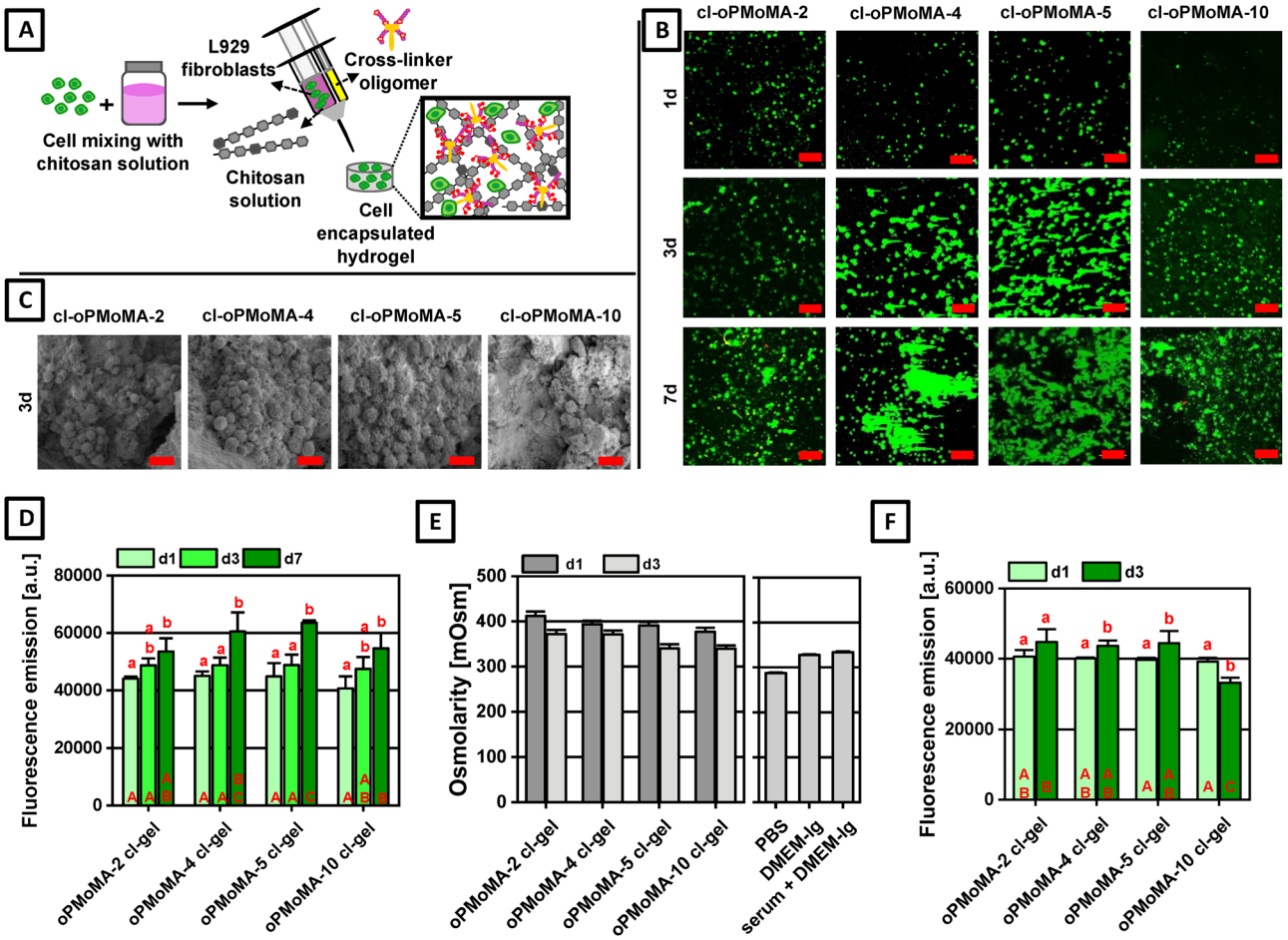

Fig. 7 (A) Schematic illustration of cell–laden injectable oligomer-cross-linked chitosan hydrogel (iCsgel) fabrication. Cytocompatibility of encapsulated L929 fibroblast cells (1×10^5 per 50 μL) in iCsgel upon cross-linking with oPMoMA-*x*. (B) Stacked CLSM images of cell–laden iCsgel at day 1, 3 and 7 after staining with Calcein-AM and EthD-1 (Live/Dead® assay) (scale bar 100 μm). (C) SEM analysis of lyophilized cell–laden iCsgel after 3 days. Scale bars represent 10 μm. (D) Metabolic activity as a measure of fluorescence emission of encapsulated L929 fibroblast cells and AlamarBlue™ reagent in iCsgel at day 1, 3 and 7. Columns with error bars represent means ± standard deviations (n = 4). Columns with different letters are statistically significantly different, small letters indicate differences within sub-group and capital letters indicate difference of respective formulations between sub-groups, $p < 0.05$. (E) Osmolarity of primary extracts (at day 1) and secondary extracts (at day 3) from cell–laden iCsgel as well as osmolarity of PBS, plain medium (DMEM-low glucose) and serum-containing medium (DMEM-low glucose 89% + FBS 10% + P/S 1%). (F) Consecutive AlamarBlue™ assay. Metabolic activity as a measure of fluorescence emission of encapsulated L929 fibroblast cells and AlamarBlue™ reagent in iCsgel at days 1 and 3. Columns with error bars represent means ± standard deviations (n = 4), small letters indicate differences within groups and capital letters indicate difference of respective formulations between groups, $p < 0.05$.

(oPMoMA and oMoMA) (Fig. S9B, left image). The blank cross-linked iCsgel (without cells) reduced yellow WST-8 to orange WST-8 formazan, therefore, data was corrected by subtracting the absorption values of control gel samples (Fig. S9B, right image). The cytocompatibility experiments clearly highlight the potential of cell–laden-hydrophilic oligomer cross-linked iCsgel in tissue engineering by facilitating viable cell encapsulation and survival.

Degradation study

The *in vitro* degradation of injectable chitosan hydrogels (iCsgel) cross-linked with various hydrophilic oligomers (oPMoMA-*x*) was conducted in PBS at 37 °C and the results were compared to non-cross-linked chitosan physical gels (Fig. 8A). The oligomer cross-linked chitosan hydrogels remained stable throughout the degradation study of 42 days, showing only slight opaqueness and shrinkage, likely due to the accumulation of buffer salts. The mass loss in the cross-linked gels was minimal, with oPMoMA-5 and oPMoMA-10 cross-linked gels being the most stable (Fig. 8B). Overall, mass loss correlated inversely with the anhydride content of the oligomer and cross-linking degree. These findings of a slow rate of degradation of cross-linked chitosan hydrogels are in general accordance with data reported for other covalently cross-linked chitosan formulations.[7,60,61] It, however, was also shown that *in vitro* degradation rate can be accelerated by adding enzymes such as lysozyme to the buffer.[62] For a more detailed insight in the hydrolytic degradation profiles of iCsgel, leachables (Fig. 8C), swelling ratio (Fig. 8D) and pH of incubation media (Fig. 8E) were monitored. Congruent with mass loss, leachables and swelling ratio from the oligomer cross-linked chitosan hydrogels were significantly less compared to non-cross-linked chitosan

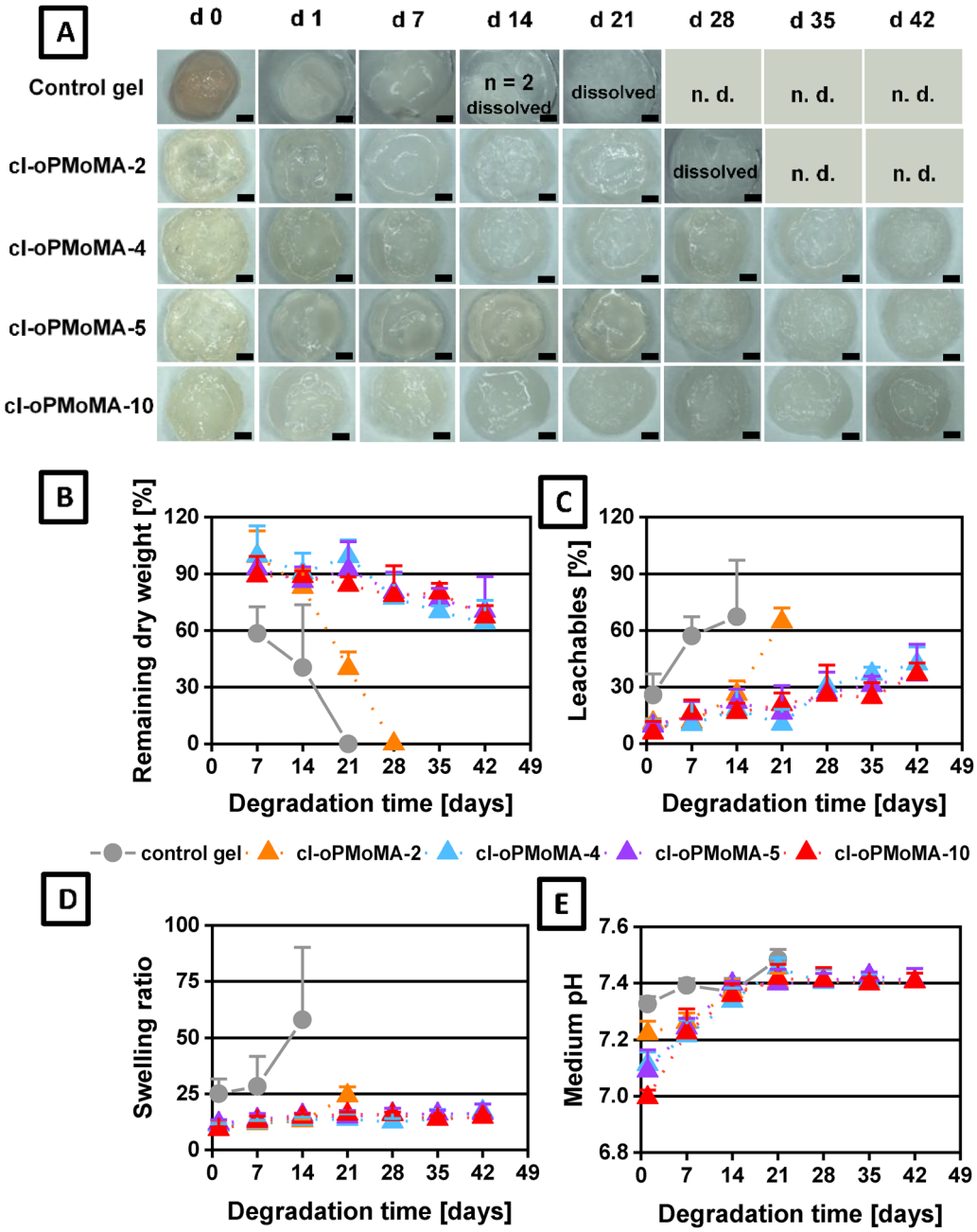

Fig. 8 Degradation characteristics of oPMoMA-*x* cross-linked iCsgel in comparison to physically gelled control in PBS at 37 °C. (A) Stereomicroscopic images of control gels and iCsgel formulations at defined degradation time points (n.d. (not determined): image missing due to complete degradation). Scale bars represent 1 mm. (B) Remaining dry weight, (C) leachables [%], (D) swelling ratio and (E) medium pH at selected degradation time points. Data points with error bars represent means ± standard deviations (n = 4).

control gels, and the pH of the incubation media remained stable over time.

Overall, our study demonstrated that these hydrophilic oligomer-cross-linked injectable chitosan hydrogels have controlled and adjustable hydrolytic degradation properties that correlate with the degree of cross-linking. In summary, the iCsgel platform appears promising to provide tailored hydrogels for the formulation of tissue engineering scaffolds suitable for cell and drug delivery applications.

Conclusion

In the present study, we have synthesized a set of hydrophilic oligomeric oligomers of low molecular weight with reactive and easily derivatizable anhydride groups that were subsequently used to covalently cross-link chitosan. Rheology revealed prompt reaction between reactive hydrophilic oligomers and chitosan. The injectable gels exhibited increased mechanical strength with increasing anhydride content of the oligomers. Generally, iCsgel exhibited a homogeneous 3D porous structure

and uniform *in vitro* degradation at a physiologically relevant rate. Moreover, iCsgel showed tuneable mechanical, swelling, and degradative properties together with excellent cytocompatibility and supported cell proliferation. In summary, the investigated hydrophilic reactive oligomer cross-linked injectable chitosan hydrogel platform is highly diverse and allows for fabrication of *in situ* tissue engineering scaffolds as well as matrices for cells and drug delivery, all with precise characteristics.

Author contributions

The defined roles of all the authors who contributed to the manuscript are in the following way: Iram Maqsood: investigation, methodology, writing, editing, and review of paper. Hafiz Awais Nawaz: investigation (particularly related to oligomers synthesis and characterization). Ketpat Vejjasilpa: some investigation related to cell culture. Caroline Kohn-Polster: some investigation related to cell culture. Jan Krieghoff: investigation related to oligomers synthesis. Alexandra Springwald: investigation related to oligomers synthesis. Michaela Schulz-Siegmund: resources, supervision, review of manuscript. Michael C. Hacker: conceptualization, funding acquisition, project administration, supervision, writing – editing and review.

Conflicts of interest

There are no conflicts to declare.

Data availability

Data supporting this article has been included in supplementary information (SI). Supplementary information: these include detailed chemical characterizations of hydrophilic oligomeric oligomers, oMoMA-*x* (Fig. S1), their compositions and chemical properties (Table S1), and analyses of anhydride content and oligomer-molecular weight correlations (Fig. S2). Rheological assessments of pristine chitosan solutions before and after autoclaving are presented (Fig. S3). Reaction conditions of chitosan solution and oligomer solution, calculation of cross-linking group ratio and corresponding storage moduli are described (Table S2). Chemical illustration of injectable oligomer-cross-linked chitosan hydrogel (iCsgel) fabrication from chitosan and reactive anhydride-containing oligomer (Fig. S4). Time-sweep rheological profiles of cross-linking reactions between chitosan and various MA-10-containing oligomers are shown (Fig. S5), supported by instrument details and kinetic data. Physico-chemical properties of iCsgel formulations, including water content and leachables, are compared to control gels (Fig. S6), stacked FTIR spectra of oPMoMA-*x* cross-linked chitosan hydrogel in comparison to pristine chitosan and β-GP (Fig. S7), representative ^{1}H NMR spectra confirming successful covalent attachment of 6-aminofluorescein (6-AF) to oPMoMA-*x* oligomers (Fig. S8) and cytocompatibility of encapsulated L929 fibroblast cells within iCsgel cross-linked with MA-5 containing oligomers is assessed through imaging and viability assays (Fig. S9). Raw data supporting all analyses can be found in the SI (Tables S3–S9). See DOI: https://doi.org/10.1039/d5tb02401c.

Acknowledgements

Financial support by the German Research Council (DFG SFB, Projektnummer 59307082/Transregio 67, project A1) as well as the personal funding from Higher Education Commission (HEC-90% overseas scholarship), Pakistan, and the German Academic Exchange Services (DAAD) to Iram Maqsood (Phase II, Batch VI) is gratefully acknowledged. We are grateful to Jörg Lenzner (Faculty of Physics and Earth Science, Leipzig University) for scanning electron microscopic (SEM) imaging. We also acknowledge Lisa Franz (Institute of Pharmacy, Pharmaceutical/Medicinal Chemistry, Leipzig University) for providing access to a Fourier transform infrared spectrophotometer (FTIR-ATR). We also thank Lothar Hennig (Department of Organic Chemistry, Leipzig University) for NMR analysis of oligomers.

References

1 F. Y. Hsieh, L. Tao, Y. Wei and S. H. Hsu, A novel biodegradable self-healing hydrogel to induce blood capillary formation, *NPG Asia Mater.*, 2017, **9**(3), 1–11, DOI: 10.1038/am.2017.23.
2 J. W. Seo, *et al.*, Injectable hydrogel derived from chitosan with tunable mechanical properties via hybrid-crosslinking system, *Carbohydr. Polym.*, 2021, **251**, 117036, DOI: 10.1016/j.carbpol.2020.117036.
3 C. D. Hoemann, J. Sun, A. Légaré, M. D. McKee and M. D. Buschmann, Tissue engineering of cartilage using an injectable and adhesive chitosan-based cell-delivery vehicle, *Osteoarthr. Cartil.*, 2005, **13**(4), 318–329, DOI: 10.1016/j.joca.2004.12.001.
4 M. Fujita, *et al.*, Vascularization in vivo caused by the controlled release of fibroblast growth factor-2 from an injectable chitosan/non-anticoagulant heparin hydrogel, *Biomaterials*, 2004, **25**(4), 699–706, DOI: 10.1016/S0142-9612(03)00557-X.
5 M. Rafat, *et al.*, PEG-stabilized carbodiimide crosslinked collagen-chitosan hydrogels for corneal tissue engineering, *Biomaterials*, 2008, **29**(29), 3960–3972, DOI: 10.1016/j.biomaterials.2008.06.017.
6 Y. Zhang, L. Tao, S. Li and Y. Wei, Synthesis of multiresponsive and dynamic chitosan-based hydrogels for controlled release of bioactive molecules, *Biomacromolecules*, 2011, **12**(8), 2894–2901, DOI: 10.1021/bm200423f.
7 F. L. Mi, Y. C. Tan, H. F. Liang and H. W. Sung, In vivo biocompatibility and degradability of a novel injectable-chitosan-based implant, *Biomaterials*, 2002, **23**(1), 181–191, DOI: 10.1016/S0142-9612(01)00094-1.

8 F. Mushtaq, *et al.*, Injectable Chitosan-Methoxy Polyethylene Glycol Hybrid Hydrogel Untangling the Wound Healing Behavior: In Vitro and In Vivo Evaluation, *ACS Omega*, 2024, **9**(2), 2145–2160, DOI: 10.1021/acsomega.3c04346.
9 M. Biernat, *et al.*, Effect of Selected Crosslinking and Stabilization Methods on the Properties of Porous Chitosan Composites Dedicated for Medical Applications, *Polymers*, 2023, **15**(11), 2507, DOI: 10.3390/polym15112507.
10 M. M. Ribeiro, M. Simões, C. Vitorino and F. Mascarenhas-Melo, Physical crosslinking of hydrogels: the potential of dynamic and reversible bonds in burn care, *Coord. Chem. Rev.*, 2025, **542**, 216868, DOI: 10.1016/j.ccr.2025.216868.
11 Z. Huang, *et al.*, Food Hydrocolloids Crosslinking strategies and functionalization modification approaches for chitosan-based hydrogels in food preservation applications: a review, *Food Hydrocolloids*, 2026, **175**, 112475, DOI: 10.1016/j.foodhyd.2026.112475.
12 P. Roughley, C. Hoemann, E. DesRosiers, F. Mwale, J. Antoniou and M. Alini, The potential of chitosan-based gels containing intervertebral disc cells for nucleus pulposus supplementation, *Biomaterials*, 2006, **27**(3), 388–396, DOI: 10.1016/j.biomaterials.2005.06.037.
13 A. Chenite, *et al.*, Novel injectable neutral solutions of chitosan form biodegradable gels in situ, *Biomaterials*, 2000, **21**(21), 2155–2161, DOI: 10.1016/S0142-9612(00)00116-2.
14 J. Berger, M. Reist, J. M. Mayer, O. Felt, N. A. Peppas and R. Gurny, Structure and interactions in covalently and ionically crosslinked chitosan hydrogels for biomedical applications, *Eur. J. Pharm. Biopharm.*, 2004, **57**(1), 19–34, DOI: 10.1016/S0939-6411(03)00161-9.
15 M. N. V. R. Kumar, R. A. A. Muzzarelli, C. Muzzarelli, H. Sashiwa and A. J. Domb, Chitosan chemistry and pharmaceutical perspectives, *Chem. Rev.*, 2004, **104**(12), 6017–6084, DOI: 10.1021/cr030441b.
16 N. Bhattarai, J. Gunn and M. Zhang, Chitosan-based hydrogels for controlled, localized drug delivery, *Adv. Drug Delivery Rev.*, 2010, **62**(1), 83–99, DOI: 10.1016/j.addr.2009.07.019.
17 N. Murata-Kamiya, H. Kaji and H. Kasai, Types of mutations induced by glyoxal, a major oxidative DNA-damage product, in Salmonella typhimurium, *Mutat. Res., Fundam. Mol. Mech. Mutagen.*, 1997, **377**(1), 13–16, DOI: 10.1016/S0027-5107(97)00016-X.
18 P. Sapuła, K. Bialik-Wąs and K. Malarz, Are Natural Compounds a Promising Alternative to Synthetic Cross-Linking Agents in the Preparation of Hydrogels?, *Pharmaceutics*, 2023, **15**(1), 253, DOI: 10.3390/pharmaceutics15010253.
19 V. A. Reyna-urrutia, V. Mata-haro and J. V. Cauich-rodriguez, Effect of two crosslinking methods on the physicochemical and biological properties of the collagen-chitosan scaffolds, *Eur. Polym. J.*, 2019, **117**, 424–433, DOI: 10.1016/j.eurpolymj.2019.05.010.
20 N. Bhattarai, H. R. Ramay, J. Gunn, F. A. Matsen and M. Zhang, PEG-grafted chitosan as an injectable thermosensitive hydrogel for sustained protein release, *J. Controlled Release*, 2005, **103**(3), 609–624, DOI: 10.1016/j.jconrel.2004.12.019.
21 A. C. Alavarse, E. C. G. Frachini, R. L. C. G. da Silva, V. H. Lima, A. Shavandi and D. F. S. Petri, Crosslinkers for polysaccharides and proteins: synthesis conditions, mechanisms, and crosslinking efficiency, a review, *Int. J. Biol. Macromol.*, 2022, **202**, 558–596, DOI: 10.1016/j.ijbiomac.2022.01.029.
22 K. Wegrzynowska-Drzymalska, *et al.*, Crosslinking of Chitosan with Dialdehyde Chitosan as a New Approach for Biomedical Applications, *Materials*, 2020, **13**(15), 1–27, DOI: 10.3390/ma13153413.
23 E. Szymańska and K. Winnicka, Stability of Chitosan—A Challenge for Pharmaceutical and Biomedical Applications, *Mar. Drugs*, 2015, **13**(4), 1819–1846, DOI: 10.3390/md13041819.
24 T. Loth, R. Hennig, C. Kascholke, R. Hötzel and M. C. Hacker, Reactive and stimuli-responsive maleic anhydride containing macromers – Multi-functional cross-linkers and building blocks for hydrogel fabrication, *React. Funct. Polym.*, 2013, **73**(11), 1480–1492, DOI: 10.1016/j.reactfunctpolym.2013.08.002.
25 C. Kascholke, *et al.*, Dual-Functional Hydrazide-Reactive and Anhydride-Containing Oligomeric Hydrogel Building Blocks, *Biomacromolecules*, 2017, **18**(3), 683–694, DOI: 10.1021/acs.biomac.6b01355.
26 M. Carpintero, I. Marcet, C. Cortizo and P. Guerrero, Food Hydrocolloids Chitosan modification with octenyl succinic anhydride (OSA): effect of the degree of substitution on the structural, mechanical and barrier properties in the synthetized bioplastics, *Food Hydrocolloids*, 2026, **171**, 111838, DOI: 10.1016/j.foodhyd.2025.111838.
27 M. Karimi, F. Ahadi, N. Esmati, M. Fan, L. Han and C. Y. Li, Heterogeneous polymerization via two-step crosslinking for tunable microribbon hydrogels, *Biofabrication*, 2026, **18**(1), 15016, DOI: 10.1088/1758-5090/ae235a.
28 H. A. Nawaz, *et al.*, Injectable oligomer-cross-linked gelatine hydrogels via anhydride-amine-conjugation, *J. Mater. Chem. B*, 2021, **9**(9), 2295–2307, DOI: 10.1039/d0tb02861d.
29 N. N. Shah, N. Soni and R. S. Singhal, Modification of proteins and polysaccharides using dodecenyl succinic anhydride: synthesis, properties and applications—A review, *Int. J. Biol. Macromol.*, 2018, **107**, 2224–2233, DOI: 10.1016/j.ijbiomac.2017.10.099.
30 N. Reddy, R. Reddy and Q. Jiang, Crosslinking biopolymers for biomedical applications, *Trends Biotechnol.*, 2015, **33**(6), 362–369, DOI: 10.1016/j.tibtech.2015.03.008.
31 T. Loth, R. Hötzel, C. Kascholke, U. Anderegg, M. Schulz-Siegmund and M. C. Hacker, Gelatin-based biomaterial engineering with anhydride-containing oligomeric cross-linkers, *Biomacromolecules*, 2014, **15**(6), 2104–2118, DOI: 10.1021/bm500241y.
32 C. Kohn, *et al.*, Dual-component collagenous peptide/reactive oligomer hydrogels as potential nerve guidance materials-from characterization to functionalization, *Biomater. Sci.*, 2016, **4**(11), 1605–1621, DOI: 10.1039/c6bm00397d.
33 C. Kohn-Polster, *et al.*, Dual-component gelatinous peptide/reactive oligomer formulations as conduit material and

luminal filler for peripheral nerve regeneration, *Int. J. Mol. Sci.*, 2017, **18**(5), 1–29, DOI: 10.3390/ijms18051104.

34 C. Kohn-Polster, *et al.*, Functionalization of Two-Component Gelatinous Peptide/Reactive Oligomer Hydrogels with Small Molecular Amines for Enhanced Cellular Interaction, *Int. J. Mol. Sci.*, 2025, **26**(11), 1–22, DOI: 10.3390/ijms26115316.

35 H. Qin, J. Wang, T. Wang, X. Gao, Q. Wan and X. Pei, Preparation and Characterization of Chitosan/β-Glycerophosphate Thermal-Sensitive Hydrogel Reinforced by Graphene Oxide, *Front. Chem.*, 2018, **6**, 565, DOI: 10.3389/fchem.2018.00565.

36 F. Eeckman, A. J. Moës and K. Amighi, Synthesis and characterization of thermosensitive copolymers for oral controlled drug delivery, *Eur. Polym. J.*, 2004, **40**(4), 873–881, DOI: 10.1016/j.eurpolymj.2003.11.010.

37 D. Filion and M. D. Buschmann, Chitosan-glycerol-phosphate (GP) gels release freely diffusible GP and possess titratable fixed charge, *Carbohydr. Polym.*, 2013, **98**(1), 813–819, DOI: 10.1016/j.carbpol.2013.06.055.

38 R. J. Krawetz, *et al.*, Collagen I Scaffolds Cross-Linked with Beta-Glycerol Phosphate Induce Osteogenic Differentiation of Embryonic Stem Cells In Vitro and Regulate Their Tumorigenic Potential In Vivo, *Tissue Eng., Part A*, 2011, **18**(9–10), 1014–1024, DOI: 10.1089/ten.tea.2011.0174.

39 H. K. No, J. W. Nah and S. P. Meyers, Effect of time/temperature treatment parameters on depolymerization of chitosan, *J. Appl. Polym. Sci.*, 2003, **87**(12), 1890–1894, DOI: 10.1002/app.11628.

40 A. San Juan, *et al.*, Degradation of chitosan-based materials after different sterilization treatments, *IOP Conf. Ser.: Mater. Sci. Eng.*, 2012, **31**, 012007, DOI: 10.1088/1757-899X/31/1/012007.

41 M. A. Torres, M. M. Beppu, C. C. Santana and E. J. Arruda, Viscous and Viscoelastic Properties of Chitosan Solutions and Gels, *Braz. J. Food Technol.*, 2006, **9**(2), 101–108.

42 E. A. El-hefian and A. H. Yahaya, Rheological study of chitosan and its blends: an overview, *Maejo Int. J. Sci. Technol.*, 2010, **4**(02), 210–220.

43 J. E. Eastoe, The amino acid composition of mammalian collagen and gelatin, *Biochem. J.*, 1955, **61**(4), 589–600.

44 S. Yang, K.-F. Leong, Z. Du and C.-K. Chua, The Design of Scaffolds for Use in Tissue Engineering. Part I. Traditional Factors, *Tissue Eng.*, 2001, **7**(6), 679–689, DOI: 10.1089/107632701753337645.

45 S. Partap, A. Muthutantri, I. U. Rehman, G. R. Davis and J. A. Darr, Preparation and characterisation of controlled porosity alginate hydrogels made via a simultaneous micelle templating and internal gelation process, *J. Mater. Sci.*, 2007, **42**(10), 3502–3507, DOI: 10.1007/s10853-007-1533-x.

46 N. Annabi, *et al.*, Controlling the porosity and microarchitecture of hydrogels for tissue engineering, *Tissue Eng., Part B*, 2010, **16**(4), 371–383, DOI: 10.1089/ten.teb.2009.0639.

47 F. Mirahmadi, M. Tafazzoli-Shadpour, M. A. Shokrgozar and S. Bonakdar, Enhanced mechanical properties of thermosensitive chitosan hydrogel by silk fibers for cartilage tissue engineering, *Mater. Sci. Eng., C*, 2013, **33**(8), 4786–4794, DOI: 10.1016/j.msec.2013.07.043.

48 I. F. Amaral, *et al.*, Fibronectin-mediated endothelialisation of chitosan porous matrices, *Biomaterials*, 2009, **30**(29), 5465–5475, DOI: 10.1016/j.biomaterials.2009.06.056.

49 D. Depan, B. Girase, J. S. Shah and R. D. K. Misra, Structure-process-property relationship of the polar graphene oxide-mediated cellular response and stimulated growth of osteoblasts on hybrid chitosan network structure nanocomposite scaffolds, *Acta Biomater.*, 2011, **7**(9), 3432–3445, DOI: 10.1016/j.actbio.2011.05.019.

50 L. Ma, *et al.*, Collagen/chitosan porous scaffolds with improved biostability for skin tissue engineering, *Biomaterials*, 2003, **24**(26), 4833–4841, DOI: 10.1016/S0142-9612(03)00374-0.

51 J. S. Mao, *et al.*, A preliminary study on chitosan and gelatin polyelectrolyte complex cytocompatibility by cell cycle and apoptosis analysis, *Biomaterials*, 2004, **25**(18), 3973–3981, DOI: 10.1016/j.biomaterials.2003.10.080.

52 S. Ladet, L. David and A. Domard, Multi-membrane hydrogels, *Nature*, 2008, **452**(7183), 76–79, DOI: 10.1038/nature06619.

53 C. M. Hwang, *et al.*, Fabrication of three-dimensional porous cell–laden hydrogel for tissue engineering, *Biofabrication*, 2010, **2**(3), 035003, DOI: 10.1088/1758-5082/2/3/035003.

54 L. Xu, C. Wang, Y. Cui, A. Li, Y. Qiao and D. Qiu, Conjoined-network rendered stiff and tough hydrogels from biogenic molecules, *Sci. Adv.*, 2019, **5**(2), eaau3442, DOI: 10.1126/sciadv.aau3442.

55 T. F. Bodoza, F. Ntuli, D. F. Chauke and E. Muzenda, The effect of poly(ethylene-*alt*-maleic anhydride) on the reduction crystallisation behaviour of nickel powder, *Can. J. Chem. Eng.*, 2013, **91**(5), 822–829, DOI: 10.1002/cjce.21753.

56 C. J. B. Alejo, C. Fasciani, M. Grenier, J. C. Netto-Ferreira and J. C. Scaiano, Reduction of resazurin to resorufin catalyzed by gold nanoparticles: dramatic reaction acceleration by laser or LED plasmon excitation, *Catal. Sci. Technol.*, 2011, **1**(8), 1506–1511, DOI: 10.1039/c1cy00236h.

57 G. V. Porcal, C. M. Previtali and S. G. Bertolotti, Photophysics of the phenoxazine dyes resazurin and resorufin in direct and reverse micelles, *Dyes Pigm.*, 2009, **80**(2), 206–211, DOI: 10.1016/j.dyepig.2008.05.014.

58 H. Vihola, A. Laukkanen, L. Valtola, H. Tenhu and J. Hirvonen, Cytotoxicity of thermosensitive polymers poly(*N*-isopropylacrylamide), poly(*N*-vinylcaprolactam) and amphiphilically modified poly(*N*-vinylcaprolactam), *Biomaterials*, 2005, **26**(16), 3055–3064, DOI: 10.1016/j.biomaterials.2004.09.008.

59 D. Cody, A. Casey, I. Naydenova and E. Mihaylova, A Comparative Cytotoxic Evaluation of Acrylamide and Diacetone Acrylamide to Investigate Their Suitability for Holographic Photopolymer Formulations, *Int. J. Polym. Sci.*, 2013, **2013**, 1–6, DOI: 10.1155/2013/564319.

60 T. Jiang, *et al.*, Chitosan-poly(lactide-*co*-glycolide) microsphere-based scaffolds for bone tissue engineering: in vitro degradation and in vivo bone regeneration studies, *Acta Biomater.*, 2010, **6**(9), 3457–3470, DOI: 10.1016/j.actbio.2010.03.023.

61 Y. Hong, H. Song, Y. Gong, Z. Mao, C. Gao and J. Shen, Covalently crosslinked chitosan hydrogel: properties of in vitro degradation and chondrocyte encapsulation, *Acta Biomater.*, 2007, **3**(1), 23–31, DOI: 10.1016/j.actbio.2006.06.007.

62 G. Lu, *et al.*, Controlling the degradation of covalently cross-linked carboxymethyl chitosan utilizing bimodal molecular weight distribution, *J. Biomater. Appl.*, 2009, **23**(5), 435–451, DOI: 10.1177/0885328208091661.